Research Article

Jaya Mohanan Jayasree Sumesh* and Maheswaran Chella Perumal

Multi-level energy efficient cooperative scheme for ring based clustering in wireless sensor network

https://doi.org/10.1515/ehs-2021-0031
Received September 27, 2021; accepted January 16, 2022;
published online April 13, 2022

Abstract: Wireless Sensor Network (WSN) is composed of different sensors attached to the same wireless medium. Sensor node data is usually forwarded to the base station, where it has been stored, evaluated, and processed. Ring Routing, a new energy-efficient distributed routing protocol aimed at larger-scale WSN applications with mobile sink and motionless sensor nodes. The structure ring is quickly converted, and they are capable of switching positions with regular nodes in a simple and effective manner, thereby minimizing the hotspot problem. In the network system, the central node is considered, and ring nodes with a certain distance are established while creating a ring structure. Since the sink nodes are powered by batteries, they deplete their batteries quicker than the other nodes, which is attributable to the accumulation of data traffic into the sink. Furthermore, when the ring configuration is disrupted due to ring node expiration, data transfer becomes tedious and causes significant delay. As a ring node starts to exhaust, its neighbor takes over as the ring node, and this selection of the regular node as the ring node is done optimally based on Multiple-Fitness Parameters such as Four-level energy consumption ($4En$), Distance (distance between the ring node and the regular node $Dist_{ring-reg}$ and distance between network centers to regular node $\Delta Dist_{C-ring}$) and delay S. Moreover, this optimal selection of the regular node to act as ring node will be carried out by a new hybrid algorithm referred to as Cuckoo Search Updated Sealion's Attacking Technique (CSUSAT) that combines the standard crow search and sea lion optimization algorithm. At last, the supremacy of the presented approach is proved over other models.

***Corresponding author: Jaya Mohanan Jayasree Sumesh**, Noorul Islam Center for higher education, Thuckalay, Kumaracoil, Tamil Nadu 629180, India, E-mail: sumeshjj15@gmail.com
Maheswaran Chella Perumal, Associate Professor, Noorul Islam Center for higher education, Thuckalay, Kumaracoil, Tamil Nadu 629180, India, E-mail: maheswaran_ncp@yahoo.co.in

Keywords: CSUSAT; defined multi-objective function; four-level energy consumption ($4E$); ring clustering; WSN.

Introduction

WSN (AlBalushi 2019; Al-Zahrani 2020; Vinitha, Rukmini, and Dhirajsunehra 2019; Yuan et al. 2019) comprises of a large series of tiny battery-powered nodes that are remotely linked throughout the wireless link (Darabkh et al. 2018; Fanian and Rafsanjani 2019; Huang, Ruan, and Meng 2018; Rathod 2020). The data has been transferred through the wireless networking medium among BS and SNs, and also between the nodes. The energy of SNs is strictly proportional to the network lifetime (Bhardwaj and Kumar 2019b; Darabkh, El-Yabroudi, and El-Mousa 2019; Movva and Rao 2019; Mythili et al. 2019; Rehan et al. 2020). During the routing period, the energy of the SNs continues to decrease (Chang and Tsai 2019; Sarkar and Senthil Murugan 2019). Further, due to the unavailability of a centralized network in the WSN, data must be transmitted from the source to destination through neighboring nodes (Fersi, Louati, and Ben Jemaa 2016; Pradeesha and Ravi 2019). Hence, it is obvious that efficient routing can enhance the network lifetime (AlBalushi 2019; Darvishi et al. 2019; Paul 2020; Vinusha and Abinaya 2018). The WSN comprise of spatially distributed independent nodes that have sensors attached to sense physical conditions such as humidity, pressure, and temperature (Sumeshb). These nodes with attached sensors finally transfer the collected data to the base station. In the transmission process energy efficiency and network lifetime are key concerns (Aseri 2013; Pandiyaraju et al. 2020; Singh and Pattanayak 2017; Zhu et al. 2020).

In WSN with a single mobile sink, ring routing is a decentralized routing protocol (Darabkh et al. 2018; Fanian and Rafsanjani 2019; Huang, Ruan, and Meng 2018; Rathod 2020). To forward the information through the network, greedy regional routing is an enticing routing approach (Al-Zahrani 2020; Bhardwaj and Kumar 2019a; Wu et al. 2019; Yuan et al. 2019). There are three nodes in the ring protocol: the ring node, the normal node, and the anchor node (Thangaramya et al. 2019; Wang 2020; Yarinezhad and Hashemi 2019). Ring Routing is based on sink location advertising to just the ring, regular nodes receiving sink position information from the ring, which is a desired one, and nodes disseminating their data through the anchor nodes, which act as intermediate actors linking the sink to the network (Dattatraya and Raghava Rao 2020; Fanian and Rafsanjani 2019; He, Long, and Zhang 2019; Rathod 2020; Tunca et al. 2013). The three sensor functions weren't fixed, which means that the sensor node will switch roles during the WSN's activity (Iztok et al. 2013; Mirjalili 2015).

The major features of ring routing are:

– Ring Routing creates an interactive ring model that enables new sink positions to be efficiently distributed to the ring and regular nodes to obtain reduced overhead as required.
– It's easy to modify the ring arrangement. The ring nodes will swap roles with normal nodes using a simple and efficient protocol, which eliminates the hotspot problem (Chithaluru, Tiwari, and Kumar 2019; Marsaline Beno et al. 2014).
– Anchor nodes along the sink's path are selected by the mobile sink, and sensor data is transmitted by the anchor nodes transmit to the sink (Thirukrishna, Karthik, and Arunachalam 2018).
– It will work with any duty-cycling, energy-aware MAC protocol (synchronized or asynchronized).
– Ring Routing can be used for either event-driven or periodic statistical analysis. It is also not query-based; therefore data is consistently transmitted as it is developed.
– Due to the easy usability of the proposed ring configuration, Ring Routing provides rapid data transmission, allowing the protocol to be used for time-sensitive applications.
– Ring Routing doesn't need any details about the sink's motion to function. It is ideal for random sink mobility situations even though it does not depend on forecasting the sink's trajectory.

Ring Routing is an energy-efficient, secure routing protocol that offers easy data transmission because of both of these characteristics (Tunca et al. 2013). The life cycle of the network continues to be reduced as the node closest to the sink node depletes even faster than the other nodes in the ring. As a result, certain parameters such as distance and delay must be considered when replacing the ring node with a regular node. Furthermore, using optimization algorithms to achieve optimum node selection will be a viable target for energy-efficient node selection (Amit and Pandey 2019; He, Long, and Zhang 2019; Jacob and Rodrigues 2019). The most interesting research works on energy-efficient RP in WSN are discussed in the literature.

The major contribution of this research work is:

– As a ring node starts to exhaust, its neighbor takes over as the ring node, and this selection of the regular node as the ring node is done optimally based on Multiple-Fitness Parameters such as Four-level energy consumption ($4En$), Distance (distance between the ring node and the regular node $Dist_{ring-reg}$ and distance between network centers to regular node $\Delta Dist_{C-ring}$) and delay S.
– The optimal selection of the regular node *reg* to act as a ring node *ring* is accomplished by a new hybrid algorithm referred as Cuckoo Search Updated Sealion's Attacking Technique (CSUSAT).

The rest of the paper is organized as: Literature review tells about the recent works done in WSN ring routing. Proposed energy-efficient ring routing protocol depicts the proposed energy-efficient ring routing protocol. Proposed ring structure formulation based on multiple-fitness parameters depicts about proposed ring structure formulation based on multiple-fitness parameters In addition, the results and conclusion are discussed briefly in Results and discussion and Conclusions.

Literature review

In 2018, Zhang et al. (2018) have proposed a "cross-layer optimization approach" for balancing the energy consumption of WSN. The authors have modeled the adopted work in such a way that the data requested throughout the networks layer be obtained from both the physical and data link layers. As a result, packet routing has become more effective. A novel energy-efficient ring cross-layer optimization algorithm as well as Leach-Cross Layer Optimization was used to observe the ring structure generated in WSN.

In 2017, Zhang et al. (2017) have addressed the energy balance problems in configured equal-area ring systems, the HRDCT solution was adopted. The researchers modeled both the clustering information announcement message and the clustering acknowledgment message using the initial RPL ("IPv6 RP for Low Power and Lossy Networks") and RFC. Also, an E2HRC RP was suggested for preserving connectivity in WSN.

In 2019, Daneshvar, Alikhah Ahari Mohajer, and Mazinani (2019) have proposed a novel clustering model that uses GWO to choose CHs. The solutions for selecting CHs were tailored based on the remaining energy of each node and the expected energy consumption. Furthermore, to improve the EE, the presented model has used equal clustering in several rounds. This prompted the system to gather the energy required to change the clustering. Finally, the results have shown that the planned model had assured a long network lifespan.

In 2020, Augustine and Ananth (2020) have proposed an improved CHS structure built on Taylor KFCM, which was adapted from the Taylor series' KFCM method. The CH was chosen by the implemented model, which has used an acceptability factor dependent on credibility, distance, and energy. Furthermore, the proposed system's benefit was demonstrated in terms of high energy and trust.

In 2019, Vinitha, Rukmini, and Dhirajsunehra (2019) have proposed the Taylor C-SSA model for energy-efficient multi-hop routing. For the Taylor, C-SSA model has been proposed for multi-hop routing. The multi-hop routing was conducted using two main stages: CH collection and data transmission. The LEACH model was used to choose the CHs in the most energy-efficient manner. Furthermore, the newly launched Taylor C-SSA has outperformed the existing models related to the picking up of the best hops.

In 2019, Darabkh, El-Yabroudi, and El-Mousa (2019) have proposed the BPA-CRP for balancing the power while routing. For power balancing, the BPA-CRP has been suggested. Furthermore, the authors have developed the RP and batch-based clustering to divide the sensor area into layers and clusters of similar scale. Furthermore, the BPA-CRP operates in its usual mode of operation, which has eliminated the discharge nodes from acting as cluster heads.

In 2019, Pradeesha and Ravi (2019) have projected the RR-MMS to minimize the overheads while ring structure formation with a clustering algorithm. Initially, the researchers have developed the ring structure based on the radius they calculated. The sink position was then modified, and the sink node location was shared among the ring structure candidates. Finally, the data was disseminated.

In 2016, Fersi, Louati, and Ben Jemaa (2016) have proposed a novel clustering technique based on the random deployment of heterogeneous WSN sensors. The CLEVER protocol was established by the developers, which has used virtual identity-based routing to achieve inter-cluster and intra-cluster connectivity. Table 1 depicts the features and challenges of existing ring based clustering techniques in WSN.

Table 1: Features and challenges of existing ring based clustering techniques in WSN.

Author [Citation]	Adopted methodology	Advantages	Drawbacks
Zhang et al. (2018)	Leach-cross layer optimization	– Ensures delivery accuracy.	– There is a need to address adverse priority problems as well as future relay-related issues. – The transmitting power is high.
Zhang et al. (2017)	HRDCT	– Reduced energy usage and network latency.	– Routing integration is high, and packet loss rates get increased.
Daneshvar, Alikhah Ahari Mohajer, and Mazinani (2019)	GWO	– Utilization of resources in such a balanced manner. – Provides the network with a long life cycle.	– Fault resistance is not considered.
Augustine and Ananth (2020)	Taylor KFCM	– Obtains increased throughput. – Minimal lag time	– Real-time tests are not taken into account.
Vinitha, Rukmini, and Dhirajsunehra (2019)	Taylor C-SSA model	– Increases the network lifespan. – Dead node pace is kept minimum.	– Insufficient throughput rate. – Reduced scalability
Darabkh, El-Yabroudi, and El-Mousa (2019)	BPA-CRP	– Each node dies smoothly with no data loss, causing no network interruption.	– Effective load balancing strategy is missing. – Decreases the number of alive nodes. – Reduces the frequency of using control messages.
Pradeesha and Ravi (2019)	RR-MMSs	– Enhances the network's lifespan. – The ring structures are easy to access.	– Successful localization is needed. – Suffers from the overhead problem.
Fersi, Louati, and Ben Jemaa (2016)	CLEVER	– Can accommodate node entry, departure, and failure with no transmitting energy wastage.	– Uses multiple nodes for data transmission, and so the network lifetime gets reduced.

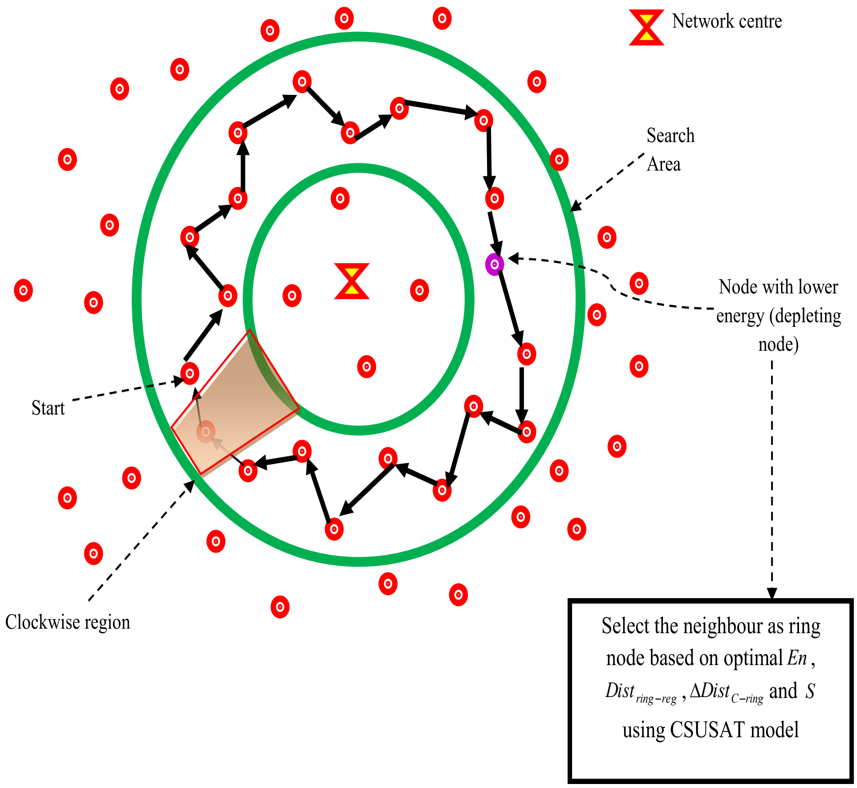

Figure 1: Ring architecture: a proposed ring node selection model.

Proposed energy-efficient ring routing protocol

The ring routing has been commonly preferred for routing the data, due to its uniform-energy consumption and delivering data in a load-balanced manner across the network. To fix the issue of data traffic in a ring routing network, an energy-efficient multi-fitness-based ring routing model is proposed, with the goal of reducing energy consumption and enhancing throughput. To limit the number of nodes within ring, the nodes transmit information to the ring nodes, and indeed the mobile sink goes across the formulated ring system and agglomerates the information. In a network system, the central node is considered, and ring nodes with a certain distance are established while creating a ring structure. Since the sink nodes are powered by batteries, they deplete their batteries quicker, which is attributable to the accumulation of data traffic into the sink. Furthermore, when the ring configuration is disrupted due to ring node expiration, data transfer becomes tedious and causes significant delay. When a ring node exhausts, its neighbor takes over as the ring node, and this selection of the regular node as the ring node is optimized under the constraints like Multiple-Fitness Parameters such as Four-level energy consumption ($4En$), Distance (distance between the ring node and the regular node $Dist_{ring-reg}$, and distance between network centers to regular node $\Delta Dist_{c-ring}$), and delay S. Moreover, this optimal selection of the regular node to act as ring node will be carried out by a new hybrid algorithm CSUSAT via considering the aforesaid constraints. A general diagrammatic representation of the proposed work is shown in Figure 1.

Proposed ring structure formulation based on multiple-fitness parameters

System model

The planned ring structure is 600 × 600 m in dimension with N count of nodes and U_n count of users, in which $n \in [N] := \{1, 2, .., N\}$. The range of node variance is set between 150 and 200 nodes. The node's communication range is set to 80 m, with a default ring radius of 150 ± 20 m. The antennas in SNs are generally Omni-directional that allows the wireless signals to propagate mostly in the shape of spherical waves. However, the signal spreads circularly in the two-dimensional plane. As a result of ring domain coordination, topology's ability successfully uses 360° signal transduction, moreover, the message collision

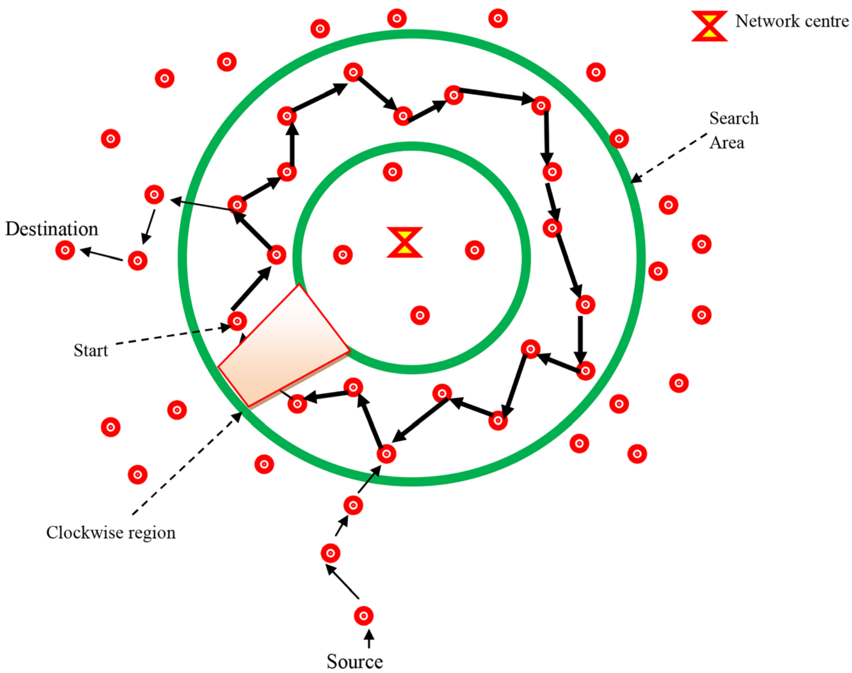

Figure 2: Data transmission via ring.

during transmission can be greatly minimized. Let's consider that ith user (source) at nth node wants to send data to jth user (destination). Initially, ith user sends his/her flow requirements to the ring node $reg_m; m = 1, \ldots, M$, which forwards the data via the ring, and finally the data will reach the jth user, who is apart from the ring. The upcoming section portrays the ring construction and our contribution towards the ring change. A diagrammatic representation of the data flow via ring is shown in Figure 2.

Ring construction

Once the WSN has been deployed, the ring structure is designed by following the steps outlined below: The network centre is established first by calculating a ring radius. The node with the highest energy forms the network center, and this node is also a part of the WSN. The ring path has been built via greedily moving nodes around the ring in a clockwise or anticlockwise direction until it completes the closed-loop. Alternatively, this procedure is rehashed among each hop, with separate neighborhood nodes being selected. It can be modified as long as the ring node lengthens its network centre. The ring structure's form irregular in shape.

Advertisement of sink position

Whenever the sink passes around the nearest neighbors, the ANs are chosen. The communication between the sensor node and the mobile sink is maintained mostly by anchor node. The sensor nodes have their known positions. Usually, the sink node selects the node with the highest energy value as its anchor node broadcasts an ANS packet to that node. Before leaving the communication range of AN, the

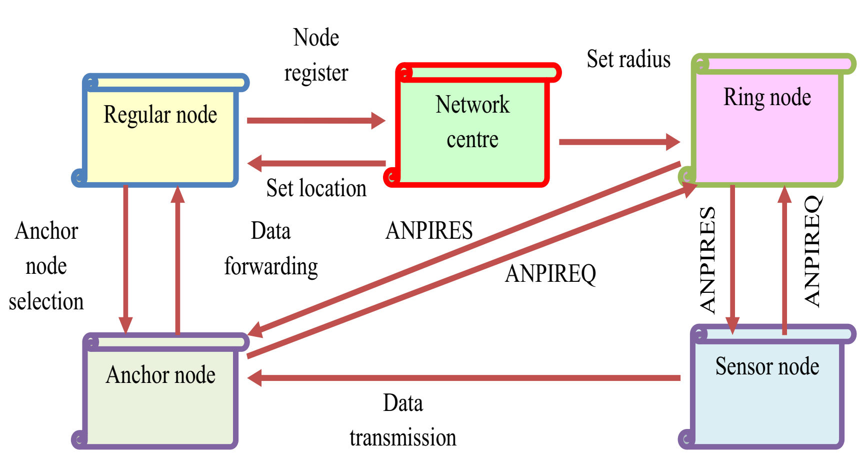

Figure 3: The flow of ring clustering.

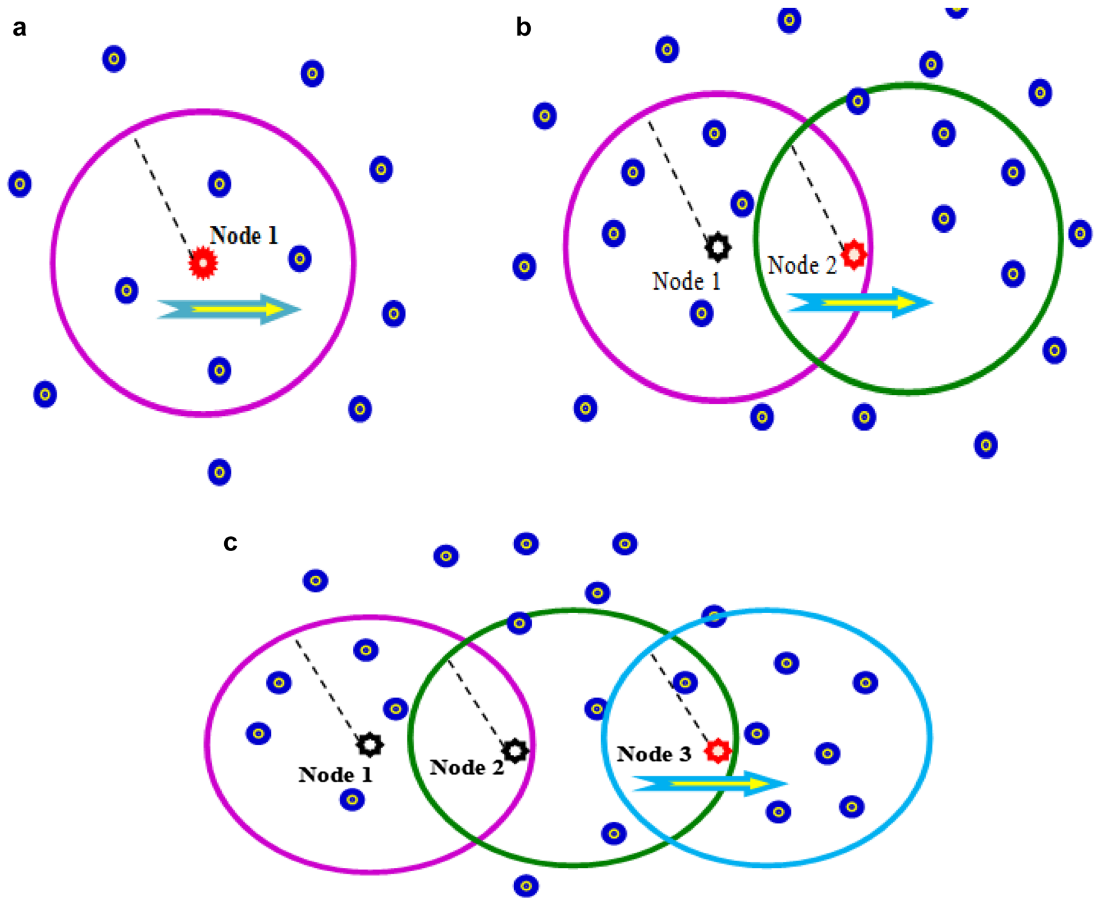

Figure 4: AN selection mechanism (a) one AN at instance of time = 1, (b) two AN at instance of time = 2, and (c) three AN at instance of time = 3.

sink selects a new AN and sends a fresh ANS packet to the old AN informing it about the new AN's location and its MAC address. Since the old AN is familiar with the new AN, data packets are being directly sent to the sink. The follow-up mechanism is the term given for this process. The AN selection is based on a resilient approach called beaconing to estimate connection consistency. The flow of ring clustering is shown in Figure 3. One of the most reliable methods for calculating link efficiency is the beconing model. In the beaconing model, the sink nodes broadcast beacon messages regularly, and the contact quality of originated reply messages from neighboring nodes is measured using a standard measurement metric (e.g. RSSI). In addition, the sink makes a decision about modifying AN based on the computed link quality estimation metric. Figure 4 depicts the AN selection process. The sink node chooses node 1 to be the AN in Figure 4(a). As node 1 goes outside the contact spectrum, node 2 is chosen as the AN, and node 2 tells node 1 about the current AN, as in Figure 4(b). When a sink moves out from the range of Node 2's contact connection, Node 3 is designated as the AN and immediately notify Node 2.

Progressive footprint chaining is used for the follow-up process and AN selection. Whenever a source node relinquishes the current AN's fixed location, it uses geographic forwarding for transmitting the information directly to the sink. If the data enters the former AN, the follow-up process transfers all those data to the sink. The MAC address and position information of new AN's are transmitted to the ring through the advertising of sink position, which sends an ANPI packet to the ring. When the AN is outside the ring, it transfers the ANPI packet to the network center. If the AN is within the ring, it uses greedy geographic forwarding to send ANPI packet to a location that is in the opposite direction of the network centre. After receiving the ANPI packet, the ring node sends an ANPIS packet towards its clockwise or counter-clockwise to the ring neighbors. The sink location advertising gets completed at this stage since all ring nodes are conscious of the MAC address and AN's position. Figure 5 shows the advertising for a sink location. As in Figure 5, ring (1) passes the "ANPI packet" throughout ring (2) to exchange the ANPI with all nodes in the ring.

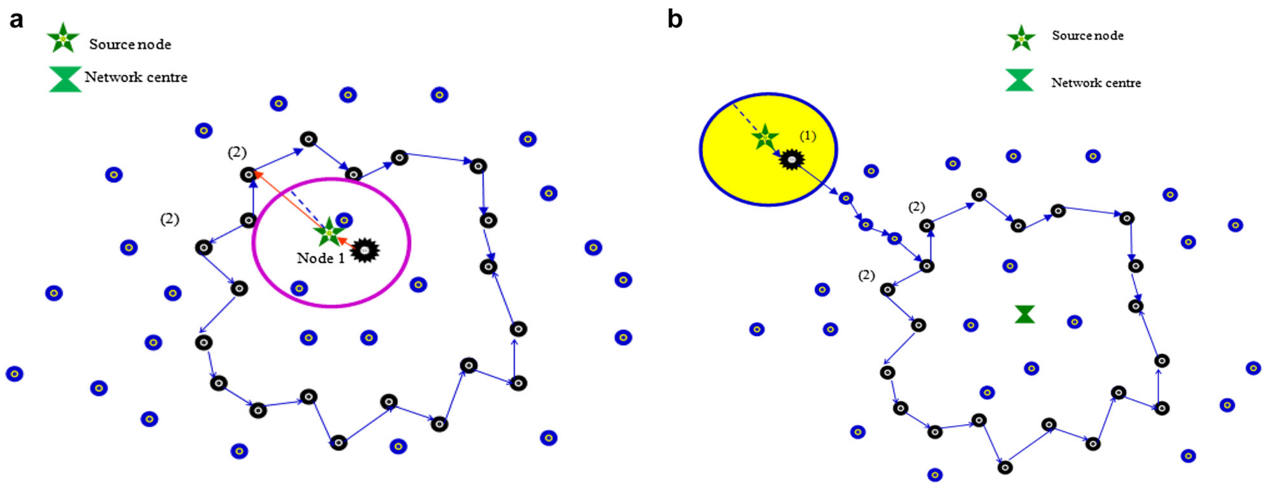

Figure 5: AN's positional advertisement where the sink is (a) on the outside of the ring and (b) on the inside of the ring.

Acquiring the ring's sink position

The source node first obtains the AN's location before disseminating the data to the sink. The AN's current location has been saved in the ring. A procedure relevant to the ANPI packets transmission to the ring is used to recover it. This mechanism is illustrated in Figure 6. The source sends the ring an ANPIREQ packet ("towards the network centre if the node is outside the ring; away from the network center if and if the node is within the ring"). Inside the packet, the source node's location is also taken into account. The ring node produces the ANPIRESP packet when it receives the ANPIREQ packet, and this ANPIRESP contains the current AN's positioning and is sent to the source node through geographic routing.

The position of the source node is also involved within the packet. The ring node on receiving the ANPIREQ packet generates an ANPIRESP packet that holds the current AN's position and delivers it to the source node by geographic routing. Once the ANPIREQ packet is received, the source node acquires the position of the AN and sends data towards it. All the intermediate nodes take the position information of AN from these packets and use it for transmitting their data to the AN. The source node acquires the AN's location and sends data to it acquiring the ANPIREQ packet. The AN's location information is extracted from all of these packets

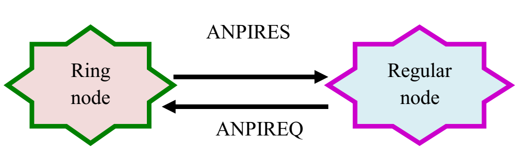

Figure 6: Flow direction of ANPIRESP and ANPIPRQ.

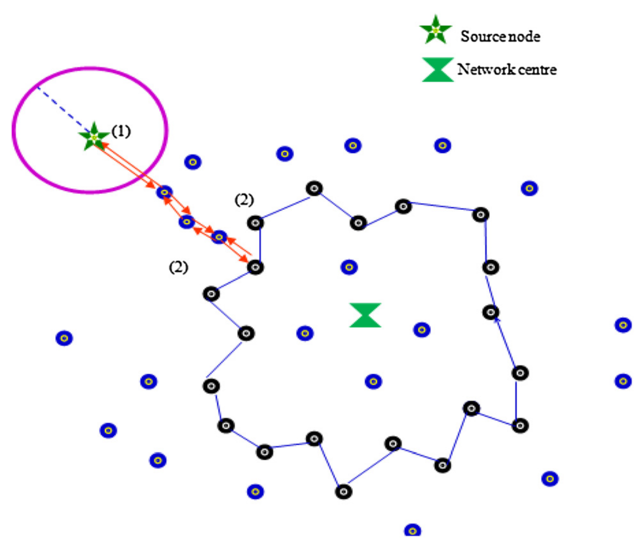

Figure 7: AN request for a location (1) and the response (2).

and all intermediate nodes send the respective information to the AN. This mechanism is shown in Figure 7.

Data dissemination

Whenever the source node receives a response (ANPIRESP) for its request (ANPIREQ), it receives the location information of AN and begins transmitting information directly to the AN through geographic forwarding. Figure 8(a) depicts this process. The follow-up process is used to disperse data to the new AN, while the data enters an older AN. This ensures that the AN has already shifted by the time, and thereby the data arrives at the destined AN. Figure 8(b) and (c) depict this operation, respectively.

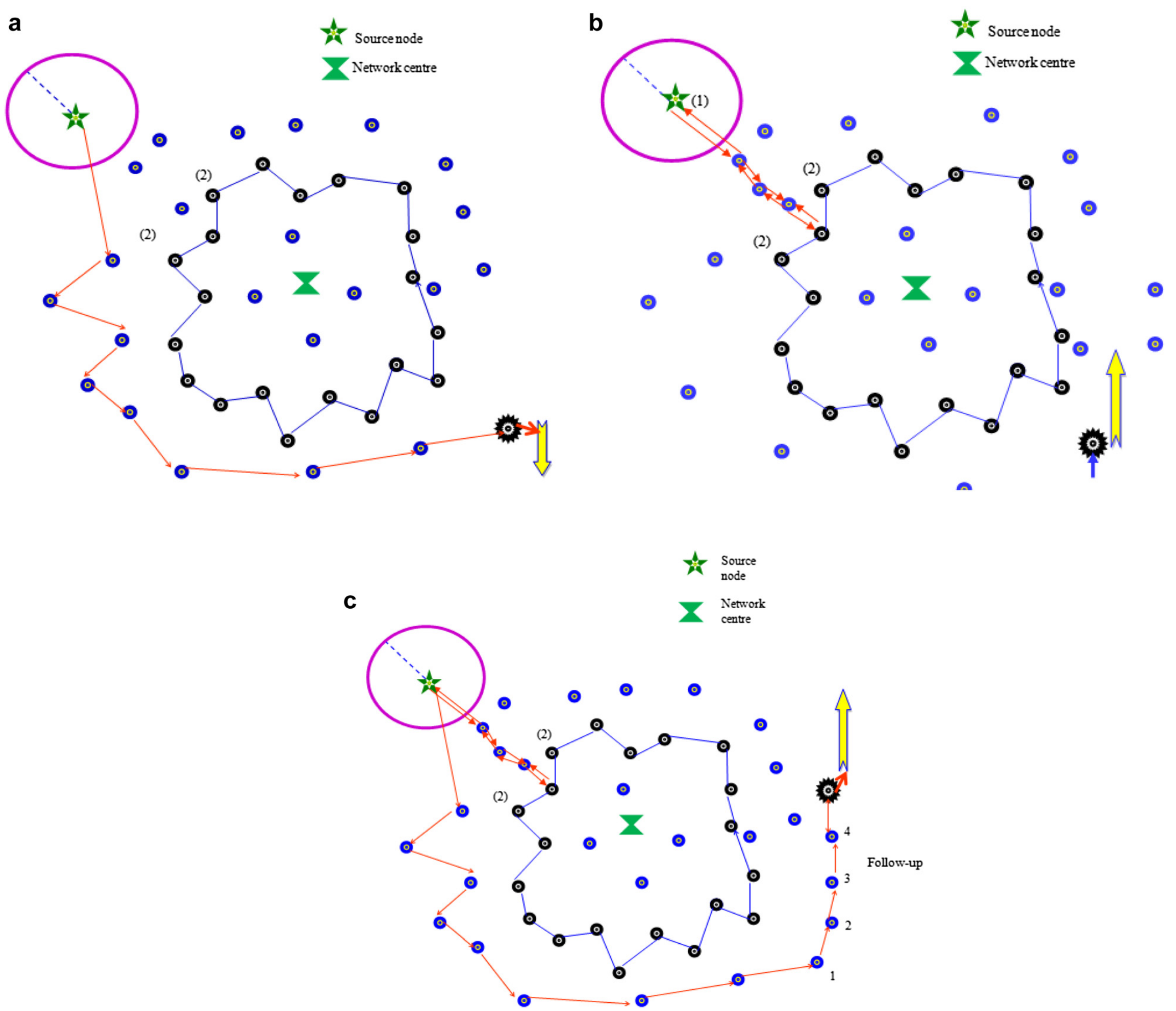

Figure 8: Shows how data is disseminated using (a) geographic forwarding, (b), and (c) follow-up mechanisms.

Ring change

In general, the ring nodes are said to consume more energy than the other nodes, and this is due to the frequent advertisement of the AN's position information and requests. Moreover, the level of traffic handled by the ring node is more general than the regular nodes. The ring nodes, therefore, tend to expire soon by losing its energy, therefore in its corresponding location, there is a need for a regular ring to act as a ring node. There is no central control entity in the WSN; therefore any of the regular nodes can switch its role as a ring node. The most interesting fact in this role switching is the selection of the optimal node, and this is considered to be the major challenge. This research work attempts to overcome this challenge using introducing a new multi-objective ring node selection model, which takes into consideration the Multiple-Fitness Parameters like four-level energy consumption, Two-level distance measure, and delay parameters. Though most of the neighbors of the expiring ring node tend to satisfy the defined Multiple-Fitness parameters, it is more crucial to select the most optimal one for efficient and ceaseless routing of data. Therefore, a new CSUSAT model is introduced for this optimal selection of the regular node to act as a ring node. The upcoming section depicts the defined multi-objective and its optimal selection mode. Figure 9 explains this mechanism.

Defined multiple-fitness parameters

The Multiple-Fitness Parameters function encompasses the four-level energy consumption, Two-level distance measure (distance between the ring and regular node &

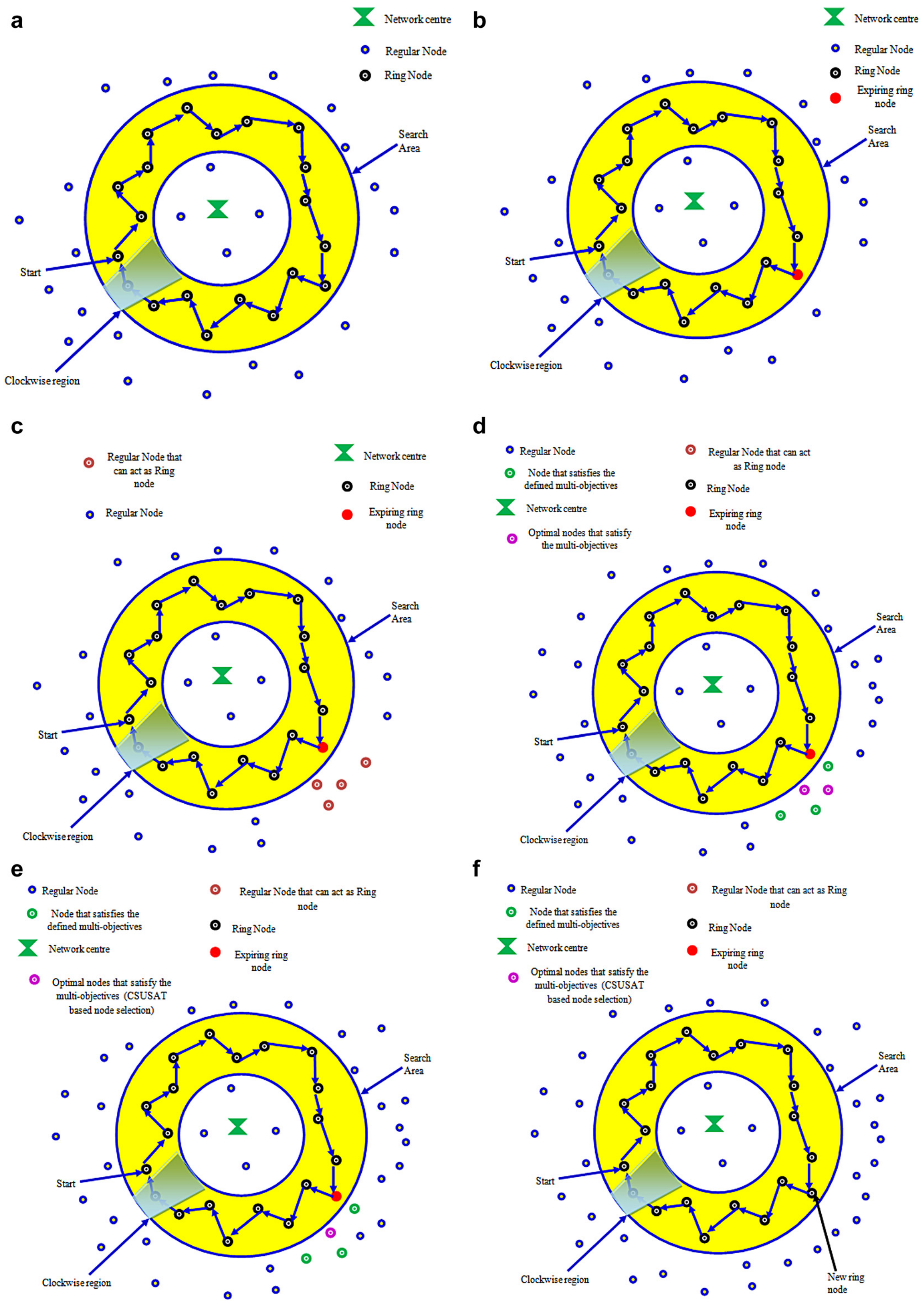

Figure 9: Choosing a regular node as a ring node, with (a) the expiring ring node, (b) peers who can be ring nodes, (c) node selection dependent on given multiple-fitness parameters, (d) optimally chosen node based on the mentioned multiple-fitness parameters, and (e) freshly constructed ring node.

distance between network centres to regular node), and delay parameters. The mathematical model of Multiple-Fitness Parameters function is represented in Eq. (1).

$$Obj = Wt_1 \times fit_q^{ene} + Wt_2 \times fit_q^{dis_{ring-reg}} + \\ + Wt_3 \times fit_q^{dis_{Nc-ring}} + Wt_4 \times fit_q^{del} \tag{1}$$

Here, Wt_1, Wt_2, Wt_3 and Wt_4 are the weight function, which is multiplied along with the fitness function to acquire more performance without getting trapped into local optima. The value of $Wt_1 = 0.4$; Wt_2, Wt_3, $Wt_4 = 0.2$. In addition, fit_q^{ene}, $fit_q^{dis_{ring-reg}}$, $fit_q^{dis_{Nc-ring}}$ and fit_q^{del} are the fitness function corresponding to the four-level energy consumption ($4E$), $Dist_{ring\ -\ reg}$, $\Delta Dist_{c-ring}$ and S

Four-level energy consumption ($4En$)**:** In WSN, energy is a limited resource. Since the senor nodes are battery powered, their life depends upon the energy factor. In real world applications, WSN is highly utilized, however the only option to enhance the applicability is by lessening the power consumption of its senor nodes. The lifetime of the sensor node is correlated with the current usage of the battery. Therefore, there is a necessity for an accurate power model.

On the other hand, in the ring network, the data dissimilation takes place only via the ring nodes, and therefore the ring node nears the sink gets expired soon. The sensor nodes being smaller in size and less expensive; therefore a regular node can switch over its role as a ring node quickly within a short span of time. Not all nodes can act as the ring node, if so there is a chance of getting distributed and the data packet forwarding potential tends to drop. Therefore, as per this research work, the node with the highest communicating energy in terms of multi-levels like residual energy (En_{res}), text level energy consumption (En_1), Image level energy consumption (En_2), video level energy consumption (En_3) will act as the ring node. The total amount of communication and the transmission distance is the overall energy expenditure. Here, En_1 is assumed to be the lowest energy level (as text data consumes less energy), and En_3 is the highest energy level (video being a continuous sequence of frames requires more energy level). The total energy of WSN En_{WSN} is the summation of En_1, En_2 and En_3 as per Eq. (2).

$$En_{WSN} = En_1 + En_2 + En_3 \tag{2}$$

During the transmission of data packets, the energy value of nodes tends to vary, and this variation is not similar for all the nodes, as they carry different types of data (any one of En_1, En_2 or En_3). On the other hand, the literary works have considered the node's energy as a constant one for any of the data transmission, therefore in such circumstance, the alive node might be considered as an expiring one. Interestingly, this works consider the node energy based on its data type, therefore the network lifetime will automatically boosted, and at the same time, the energy of the nodes can be determined more accurately based on its transmission performance. The energy En_1, En_2 and En_3 includes the transmission energy En_{TX1}, En_{TX2}, En_{TX3}, reception energy En_{RX1}, En_{RX2}, En_{RX3}, required energy during the idle state $En_{I,}$ and energy cost during sensing En_B. The mathematical formula for En_1, $En_2 En_3$ is depicted below as per Eqs. (3)–(5).

$$En_1 = En_{TX(1)} + En_{RX(1)} + En_{I(1)} + En_{B(1)} \tag{3}$$

$$En_2 = En_{TX(2)} + En_{RX(2)} + En_{I(2)} + En_{B(2)} \tag{4}$$

$$En_3 = En_{TX(3)} + En_{RX(3)} + En_{I(3)} + En_{B(3)} \tag{5}$$

In which,

$$En_{TX(1)}(P_i : d) = \begin{cases} En_{el(1)} * P + En_{fs(1)} * P * d^2, if \ \ d < d_0 \\ En_{el(1)} * P + En_{pw(1)} * P * d^4, if \ \ d \geq d_0 \end{cases} \tag{6}$$

$$En_{TX(2)}(P_i : d) = \begin{cases} En_{el(2)} * P + En_{fs(2)} * P * d^2, if \ \ d < d_0 \\ En_{el(2)} * P + En_{pw(2)} * P * d^4, if \ \ d \geq d_0 \end{cases} \tag{7}$$

$$En_{TX(3)}(P_i : d) = \begin{cases} En_{el(3)} * P + En_{fs(3)} * P * d^2, if \ \ d < d_0 \\ En_{el(3)} * P + En_{pw(3)} * P * d^4, if \ \ d \geq d_0 \end{cases} \tag{8}$$

Here, $En_{TX(1)}(P_i : d)$, $En_{TX(2)}(P_i : d)$ and $En_{TX(3)}(P_i : d)$ is the total energy required for transmitting En_1, En_2 and En_3 respectively. In addition, d and P points to the distance and the count of data packets, respectively. The energy consumed for transmitting per bit data in En_1, En_2 and En_3 is denoted as $En_{el(1)}$, $En_{el(2)}$ and $En_{el(3)}$, respectively. In addition, $d_0 = \sqrt{\frac{En_{fs}}{En_{pw}}}$ is the threshold distance. The value of $En_{TX(1)}(P_i : d)$, $En_{TX(2)}(P_i : d)$ and $En_{TX(3)}(P_i : d)$ is fixed as 50*0.000000001, and $En_{el(1)}$, $En_{el(2)}$ and $En_{el(3)}$ is 0.0013*0.000000000001. In addition, $En_{fs(1)}$, $En_{fs(2)}$, $En_{fs(3)}$ is free-space data transfer energy and it is fixed as 10*0.000000000001. Moreover, $En_{pw(1)}$, $En_{pw(2)}$, $En_{pw(3)}$ is the power amplification of En_1, En_2 and En_3. The amplification energy of En_1, En_2 and En_3 is denoted as $En_{am(1)}$, $En_{am(2)}$ and $En_{am(3)}$, respectively. This is mathematically shown in Eqs. (9)–(11) for En_1, En_2 and En_3, respectively.

$$En_{am(1)} = En_{fs(1)} d^2 \tag{9}$$

$$En_{am(2)} = En_{fs(2)} d^2 \tag{10}$$

$$En_{am(3)} = En_{fs(3)} d^2 \tag{11}$$

At the receiver side, the energy consumed for receiving the same P count of data packets for transmitting En_1, En_2 and En_3 is defined as per Eqs. (12)–(14).

$$En_{RX(1)}(P:dis) = En_{el(1)}.P \tag{12}$$

$$En_{RX(2)}(P:dis) = En_{el(2)}.P \tag{13}$$

$$En_{RX(3)}(P:dis) = En_{el(3)}.P \tag{14}$$

In addition, the residual energy En_{res} is considered, and it is mathematically given in Eq. (15). Here, En_{total} is initial energy of the network.

$$En_{res} = En_{total} - En_{WSN} \tag{15}$$

Further, the fitness function of En_{res} is expressed in Eq. (16), in which $fit^{ene}_{(a)}, fit^{ene}_{(a)}$ assumes the energy fitness to be maximal.

$$fit^{ene}_{q} = \frac{fit^{ene}_{(a)}}{fit^{ene}_{(b)}} \tag{16}$$

The functions fit_a and fit_b can be determined for E_{res} using Eqs. (17) and (18), respectively. Here, β lies between $0 < \beta < 1$, and σ_1, σ_2 and σ_3 are the constant parameters corresponding to En, dis_{r-r} and dis_{C-R}, respectively. In addition, $\sigma_1 + \sigma_2 + \sigma_3 = 1$

$$fit_a = \sigma_1 * fit^{Dis_{r-r}}_{i} + \sigma_2 * fit^{EN_{r-r}}_{i} + \sigma_3 * fit^{dis_{NC-R}}_{i} \tag{17}$$

$$fit_b = \frac{1}{n}\sum_{x=1}^{n} \|N^x - B_s\| \tag{18}$$

Two-level distance model (*dis*)**:** Distance is another essential measure, which needs to be precisely measured. In this research work, two-level distance: distance between the ring node and the regular node $Dist_{ring-reg}$ and distance between network centres to regular node $\Delta Dist_{C-ring}$ is computed. The regular node that satisfy the minimal value of $\Delta Dist_{C-ring}$ and $Dist_{ring-reg}$ is considered to be the appropriate node to act as the ring node. The distance matrix $DM(m*n)$ for the distance between *ring*, *reg* nodes is given as per Eq. (19).

$$DM(m*n) = \begin{bmatrix} dis_{NO_{ring1,reg1,}} dis_{NO_{ring2,reg2}} \ldots\ldots\ldots dis_{NO_{ringn-regn}} \\ dis_{NO_{ring1,reg1}} dis_{NO_{ring2,reg2}} \ldots\ldots\ldots dis_{NO_{ringn,regn}}. \\ : \\ : \\ dis_{NO_{ring\,m,reg1}} dis_{NO_{ring\,m,reg1}} \ldots\ldots\ldots dis_{NO_{ringm,regn}} \end{bmatrix} \tag{19}$$

The distance matrix $DM\,(m*n)$ is given as per Eq. (20) for the distance among $N - reg$ nodes.

$$DM(m*n) = \begin{bmatrix} Dist_{NO_{Nc1-reg1,}} Dist_{NO_{Nc2-reg2}} \ldots\ldots\ldots Dist_{NO_{Nc2-regn}} \\ Dist_{NO_{Nc1-reg1}} Dist_{NO_{Nc2-reg2}} \ldots\ldots\ldots Dist_{NO_{Ncn-reg2}}. \\ : \\ : \\ Dist_{NO_{Nc1m-reg1}} Dist_{NO_{Ncm-reg2}} \ldots\ldots\ldots Dist_{NO_{Ncm-regn}} \end{bmatrix} \tag{20}$$

The Euclidean distance among *reg* and *ring* located at *x*, *y* location is defined as per Eq. (21). The Euclidean distance computation among *N* and *ring* located at *p*, *r* location is defined as per Eq. (22).

$$Dist_{x,y} = \sqrt{\left(ring_y - reg_y\right)^2 + \left(ring_x - reg_x\right)^2} \tag{21}$$

$$Dist_{p,q} = \sqrt{\left(ring_p - reg_r\right)^2 + \left(ring_p - reg_r\right)^2} \tag{22}$$

The fitness function of distance $Dist_{ring-reg}$ is shown in Eqs. (23)–(25), respectively.

$$fit^{dis_{ring-reg}}_{q} = \frac{fit^{Dist_{ring-reg}}_{(a)}}{fit^{Dist_{ring-reg}}_{(b)}} \tag{23}$$

$$fit^{Dist_{ring-reg}}_{(a)} = \sum_{x=1}^{No_{ring}} \left[\| Cen_x - B_s \| + \sum_{y=1}^{No_{ring}} \|Cen_x - X_x\| \right] \tag{24}$$

$$fit^{Dist_{ring-reg}}_{(b)} = \sum_{x=1}^{No_{ring}} \sum_{y=1}^{No_{reg}} \|Cen_x - X_y\| \tag{25}$$

The fitness function of distance $Dist_{c-ring}$ is shown in Eqs. (26)–(28), respectively. Here, Cen_x refers to the *x*th network centre.

$$fit^{Dist_{Nc-ring}}_{q} = \frac{fit^{Dist_{Nc-ring}}_{(a)}}{fit^{Dist_{Nc-ring}}_{(b)}} \tag{26}$$

$$fit^{Dist_{Nc-ring}}_{(a)} = \sum_{p=1}^{No_{Nc}} \left[\| Cen_x - B_p \| + \sum_{y=1}^{No_{Nc}} \|Cen_x - X_p\| \right] \tag{27}$$

$$fit^{Dist_{Nc-ring}}_{(b)} = \sum_{p=1}^{No_{Nc}} \sum_{q=1}^{No_{ring}} \|Cen_x - X_q\| \tag{28}$$

Delay: The node with least delay is considered to be the most appropriate node to act as ring node. In general, the delay of the node is correlated with the total count of nodes in the ring. The fitness function of delay is given in Eq. (29). The value of f^{del}_{i} must be within the range [0, 1].

$$fit^{del}_{q} = \frac{\max\left(\| Cen_x - X_x \|\right)^{N_c}_{x=1}}{reg_m} \tag{29}$$

Moreover, there is chance for multiple nodes to satisfy the defined multi-objective function. In such a situation, it is crucial to select the most appropriate node. In these days, the optimization algorithms are found to be good in finding the global solutions without getting trapped into the local optima. On the other hand, the Hybrid optimization algorithms are said to be better than conventional algorithms in enhancing the convergence speed (Marsaline Beno et al. 2014). Therefore, in this research work, CSUSAT

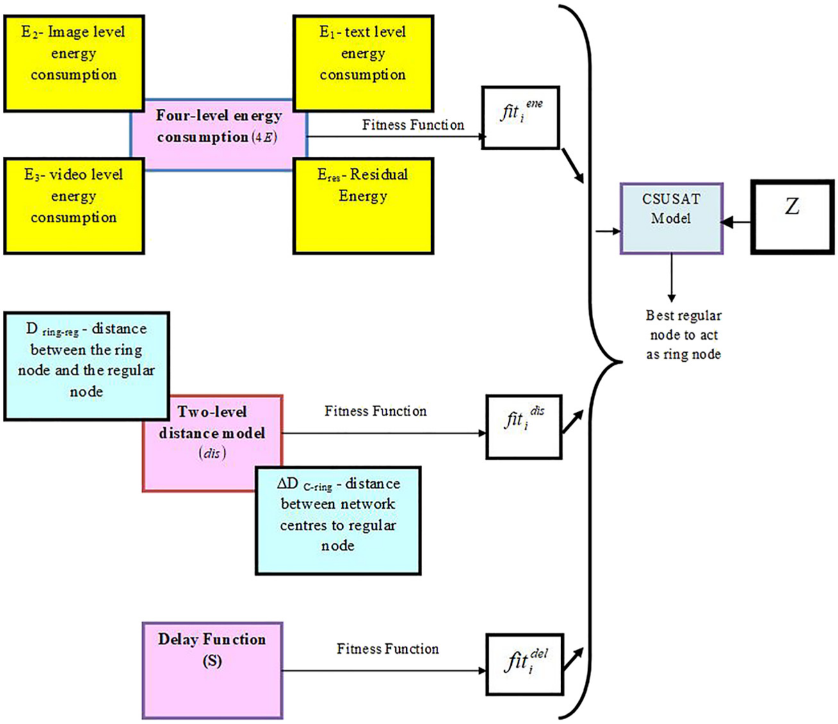

Figure 10: Considered multi-fitness parameters and solutions given to CSUSAT model.

model is introduced for optimal selection of the regular node to act as ring node. The considered multi-objectives and the solution given to proposed CSUSAT model is shown in Figure 10.

CSUSAT model

The CSA is focused on the flock of crows' intelligent behavior. CSA is usually considered to be very useful in solving complex engineering-related optimization problems. Furthermore, the SLnO model is built on sea lion hunting behavior has a higher convergence, and is better at identifying global solutions without getting stuck in local optima. The hybrid optimization algorithms are good in exploring the most optimal solutions with higher convergence and precision (Marsaline Beno et al. 2014). Therefore, the SLnO model and CSA model is hybridized in this research work. The steps followed in the proposed optimization model are depicted below:

i. Initialize the population P of the search agent. The position of the search agent is given as $Z_i = Z_1, Z_2, Z_3, \ldots, Z_I$ (regular nodes). Here, I denotes the overall count of search agents. The current iteration is pointed as *iter*, and the overall count of iterations is represented as Max^{iter}.

ii. Assign the position of a flock of G crows randomly in the search space

iii. Estimate the position of the D crows

iv. Assign the memory k of every crow

$$Memory = \begin{bmatrix} k_1^1 & k_2^1 & \ldots & k_u^1 \\ k_1^2 & k_2^2 & \ldots & k_u^2 \\ \vdots & \vdots & \ldots & \vdots \\ k_1^K & k_2^K & \ldots & k_u^K \end{bmatrix} \tag{30}$$

v. while $iter < Max^{iter}$ do

vi. for $D = 1{:}G$

vii. Compute the fitness function using Eq. (1)

viii. Select any one crow randomly to follow the D crow (for instance E)

ix. Fix awareness probability AP of crow E at *iter* as $AP^{E,\,iter}$

x. As per the proposed logic, if $R_E \geq AP^{E,\,iter}$, then compute Z^{iter+1} as per the newly formulated position update given in Eq. (31). In the below expression, the inertial weight w_{iter} is introduced to explore more precise solutions within the solution bounds.

$$Z^{D,\,iter+1} = \begin{cases} Z^{D,\,iter} \times w_{iter} + R^D \times fl^{iter} \times \left(m^{E,\,iter} - X^{D,\,iter}\right) & R_E \geq AP^{D,\,iter} \\ a\ random\ position & Otherwise \end{cases} \tag{31}$$

Here,

$$w_{iter} = w_{\max} - (w_{\max} - w_{\min}) \times \frac{iter}{Max^{iter}} \quad (32)$$

The hiding position of the crow D is depicted by $m^{D,\,iter}$ at $iter$. In addition, fl^{iter} specifies the flight length of the crow i at t and RD signifies an arbitrary integer. In addition, $w_{\max}$ and $w_{\min}$ are the maximal and minimal values of inertial weights. Moreover, w_{iter} is large, when the search space is large.

i. As per the proposed logic, if $R_E < AP^{E,\,iter}$, update the position of the search agent using the attacking phase of SLnO model. The attacking mechanism of a sea lion is defined in Eq. (21), where $H(iter) - Z(iter)$ denotes the distance between the sea lion and the target prey, || denotes the absolute value, and l denotes the random number between 0 and 1. In this research, the cosine value in Eq. (33) is computed using COSINE algorithm.

$$Z^{D,\,iter+1} = \left(\left|H^{D,\,iter} - Z^{D,\,iter}.\cos(2\pi l)\right| + H^{D,\,iter}\right) \quad (33)$$

ii. Compute the fitness function using Eq. (1)
iii. Verify the viability of novel positions.
iv. Calculate fitness of novel positions.
v. Memory is updated
vi. Return $Z^{D,iter+1}$ as the best position

Algorithm 1: Pseudocode of CSUSAT

Z is the input.
Fix Z^{iter+1} as an output
Assign a flock of G crows to a random location in the search space.
Approximate the crows' location.
Allocate each crow's memory
while $iter < iter_{\max}$
for $D = 1{:}G$
To follow D, choose any crow at random (for instance E)
Fix awareness probability
if $R_E \geq AP^{E,\,iter}$
Compute the new position of the search agent using Eq. (31).
else
Compute the new position of the search agent using Eq. (33).
end if
end for
Confirm that new vacancies are possible.
Approximate the crows' new positions.
Update the crow memory
end while

Results and discussion

Simulation procedure

MATLAB implementation was carried out. An experimental assessment is performed in terms of the number of alive nodes, throughput, and transmission delay, and the results are reported. This assessment was made by contrasting the proposed study (CSUSAT) with existing researches such as SA-DHO (Sumesha), MIFA (Rehan et al. 2020), SLnO, CSA, and Ring Routing (Tunca et al. 2013), respectively. The evaluation of the projected work is made in terms of two scenarios: Scenario 1 (fixing 150 count of nodes) and Scenario 2 (fixing 200 count of nodes). Table 2 shows the simulation parameters.

Analysis on count of alive nodes

At each round of the routing mechanism, the number of alive nodes decreases. When nodes reach the end of their life, they must be replaced by the new one. Based on the multi-objective, the new node will be selected, and it takes the place of the expiring nodes. Furthermore, the count of alive nodes is analyzed for both the scenarios (Scenarios 1 and 2) for proposed and traditional models (Figure 11). The research is carried out for varying node count sets namely 150, 200, 250, and 300, respectively. From the recorded results, a clear conclusion can be derived that the alive nodes is higher with the proposed work than the existing models. To add extra value to this assessment, a mathematical evaluation is made. In case of Scenario 1, the proposed work is 6.6, 10, 5.3, 4.6 and 93.3% superior to the existing models like SA-DHO (Sumesha), MIFA (Rehan et al. 2020), SLnO, CSA and Ring Routing (Tunca et al. 2013), respectively, for count of nodes = 150 (In Figure 11(a)). On the other hand, in case of scenatio2, the proposed work had maintained more alive nodes. In case of Scenario 2 at count of nodes = 300, the proposed work is 11.65, 12.3, 8.3, 15 and 96.6% superior to the existing models like SA-DHO (Sumesha), MIFA (Rehan et al. 2020), SLnO, CSA and Ring Routing (Tunca et al. 2013), respectively (In Figure 11(b)). Moreover, in both these analyses, it is vivid that the proposed work had more alive nodes at the

Table 2: Simulation paramerters.

Parameters	Values
Nodes	150, 200, 250, 300
Transmitter/receiver electronics	Etx = Erx = 50*0.000000001
No of messages to passed in each node variations	2000
Ring radius from center node	150

highest count of rounds. As the life span of the node is based on the energy consumption of data they transfer, i.e., residual energy (E_{res}), text level energy consumption (E_1), Image level energy consumption (E_2), video level energy consumption (E_3), the nodes do not lose the energy in an equivalent manner. This energy level calculation during communication makes the dead node approximation more appropriate. From this evaluation, it is clear that the proposed work is the energy-efficient ring routing model.

Analysis on network lifetime

The life span of the network seems to be the major issue with most of the literature works (Darabkh, El-Yabroudi, and El-Mousa 2019; Pradeesha and Ravi 2019; Vinitha, Rukmini, and Dhirajsunehra 2019). By taking this as a challenge, the proposed work has attempted to expand the network life span. To validate the proposed work in terms of life span, the evaluation is made between the proposed as well as existing works by varying the count of nodes such as 150, 200, 250, and 300. As per the recorded results, the life span of the network seems to be higher with the proposed work. This enhancement is due to the increase in the alive nodes count as well as energy efficiency. In case of Scenarios 1 and 2, the proposed work has recorded the highest network life span. In case of scenrio1 at node count = 300, the life span of the proposed work is 20, 18, 17, and 26% superior to the existing models like SA-DHO (Sumesha), MIFA (Rehan et al. 2020), SLnO and CSA respectively (In Figure 12(a)). Similar to this, the life span of the proposed work is higher in case of Scenario 2 as well. Here, the proposed work is 20, 19, 17.5, 16.75% superior to the existing models like SA-DHO (Sumesha), MIFA (Rehan et al. 2020), SLnO and CSA respectively (In Figure 12(b)). In both these cases, the highest life span is recorded with more node count. Altogether, the performance of the proposed work remains efficient in improving the network lifetime with the proposed optimal solution.

Analysis on residual energy

The leftover or residual energy after E_{WSN} dissipation is investigated in this section. Figures 13 and 14 illustrate the

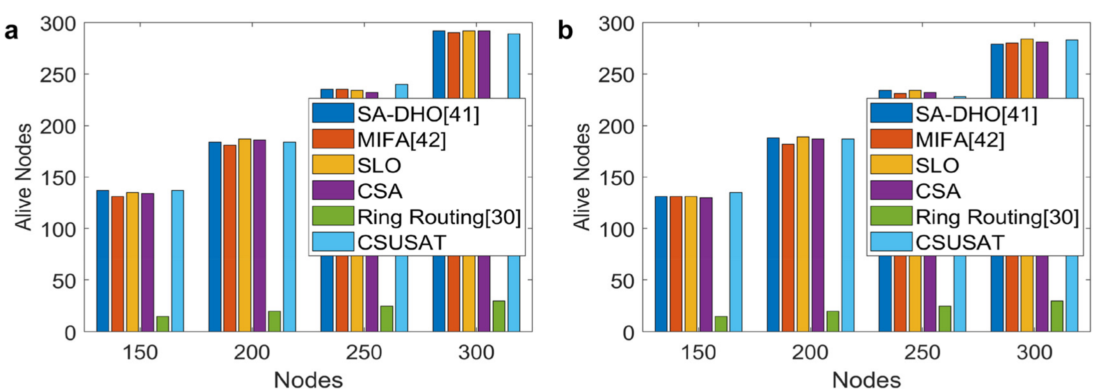

Figure 11: Analysis on count of alive nodes of CSUSAT model (a) Scenario 1 and (b) Scenario 2.

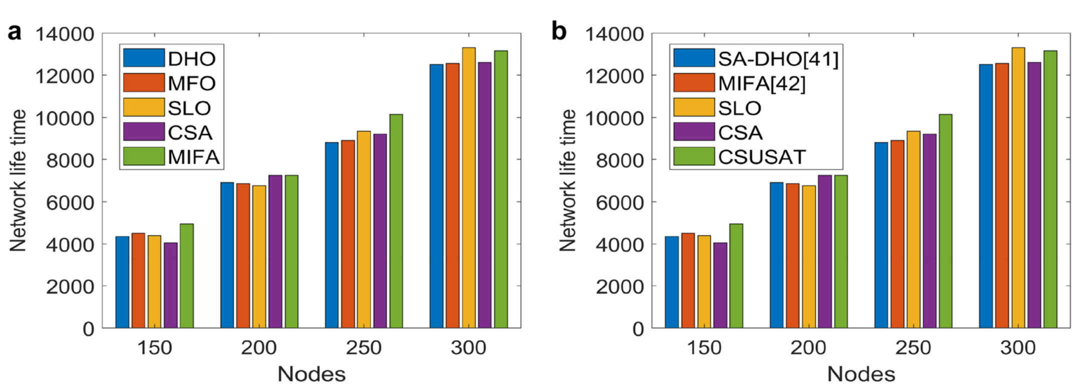

Figure 12: Analysis on network lifetime of CSUSAT model in terms of (a) Scenario 1 and (b) Scenario 2.

schematic effects of residual energy analysis for both the proposed and standard versions in case of Scenarios 1 and 2, respectively. This evaluation is performed by varying the number of messages sent from 0 to 500, 1000, 1500, and 2000. It is claimed that the model with the highest residual energy is more energy efficient. The proposed model attains this requirement, and it is said to be more energy efficient even with any difference in message quantity transfer (any one of E1, E2 or E3). On the basis of a count of message = 2000 for Scenario 1, the proposed work is 12.5, 7.5, 10.2, 5.1 and 75% better than the existing models like SA-DHO (Sumesha), MIFA (Rehan et al. 2020), SLnO and CSA respectively (In Figure 13(a)). On observing Scenario 2 for 250 counts of nodes, the proposed work has achieved the highest residual energy as 1.75 J/ which is the highest value when compared to the existing models. Similarly, when the number of nodes is 200, 250, or 300, the presented work has the maximum residual capacity, even when 2000 messages are sent. As a consequence of the overall assessment, it is clear that the proposed work has attained more residual energy, and hence the suggested methodology extends the lifetime of the network.

Throughput analysis

In general, the throughput T is the ratio of the received data $Data^{rec}$ to the actual data $Data^{actual}$. It is shown in Eq. (35).

$$T = \frac{Data^{rec}}{Data^{actual}} \tag{35}$$

For a standardized data communication system, data loss during transmission must be minimized. The system's throughput would be higher if the data loss is lower. Tables 3 and 4 show the throughput results for the proposed and existing models in case of Scenarios 1 and 2, respectively. In case of case of Scenario 2, the proposed work had achieved the highest throughput as 11,579, which is superior to SA-DHO = 11,141, MIFA = 11,127, SLnO = 11,105, and CSA = 11,167, when the count of nodes = 150. On the other hand, in case of Scenario 2, the proposed work is 6.085, 5.3165, 7.143, and 6.517% better than the existing models like SA-DHO, MIFA, SLnO, and CSA respectively. According to the overall assessment, the presented research has the fastest throughput and the shortest data transfer delay. However, for the proposed work, the number of messages sent is more. This demonstrates that data loss is pretty

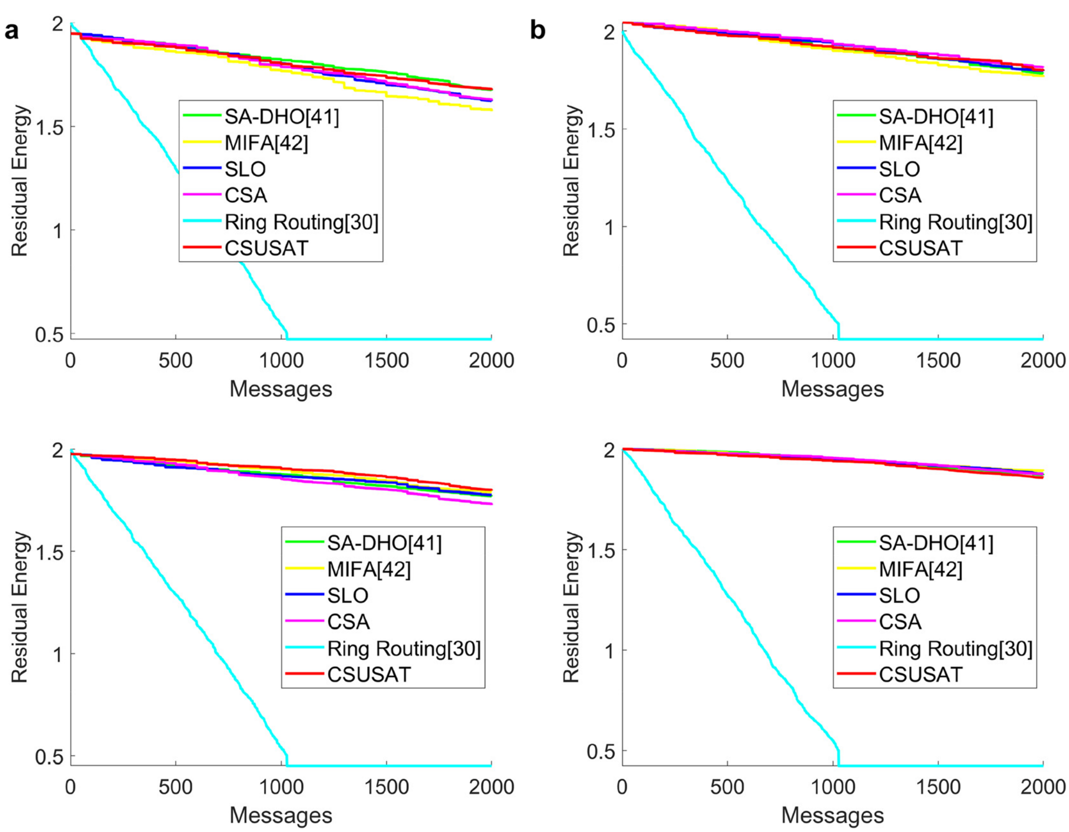

Figure 13: Analysis on residual energy of Scenario 1 at (a) count of node = 150, (b) count of nodes = 200.

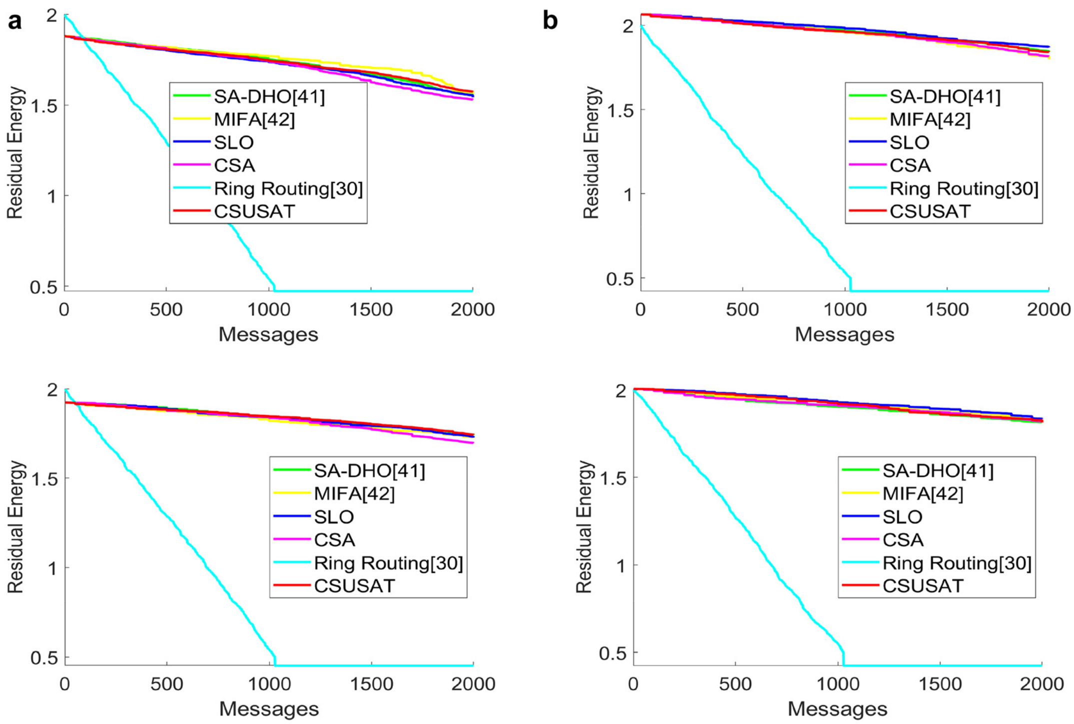

Figure 14: Analysis on residual energy of Scenario 2 at (a) count of node = 150, (b) count of nodes = 200.

uncommon, and therefore the throughput might be lower in certain rare cases.

Table 3: Analysis on throughput under Scenario 1.

Count of nodes	SA-DHO (Sumesha)	MIFA (Sumeshb)	SLO	CSA	CSUSAT
150	11,141	11,127	11,105	11,167	11,579
200	10,986	11,193	11,129	11,164	11,399
250	10,143	10,229	10,341	9986.4	10,638
300	10,639	10,521	10,664	10,534	10,783

Analysis on transmission delay

The transmission delay Tr^{delay} is computed using Eq. (36), where P^{size} is the packet size and Tr^{rate} is the transmission rate (mbps). In this research work, Tr^{rate} is fixed as 10 mbps.

$$Tr^{delay} = \frac{P^{size}}{Tr^{rate}} \tag{36}$$

Tables 5 and 6 show the packet transmission delay of the proposed and existing work for various node counts under Scenarios 1 and 2, respectively. In case of Scenario 1, the proposed work had recorded the lowest delay than the existing techniques like SA-DHO, SLnO, and CSA, respectively.

Conclusions

In this research work, an energy-efficient ring node routing model was introduced. The selection of the common node as the ring node is made optimally based on Multiple-Fitness Parameters. Moreover, the optimal selection of the regular node is performed by a novel hybrid algorithm named as CSUSAT. Accordingly, the supremacy of the presented approach is proved with respect to varied measures like count of alive nodes, residual energy, and network life span. In the case of scenrio1 at node count = 300, the life span of the proposed work is 20, 18, 17 and 26%, superior to the existing models like SA-DHO (Sumesha), MIFA (Rehan et al. 2020), SLnO and CSA, respectively. Similar to this, the life span of the proposed work is higher in the case of Scenario 2 too. In case of

Table 4: Analysis on throughput under Scenario 2.

Count of nodes	SA-DHO (Sumesha)	MIFA (Sumeshb)	SLO	CSA	CSUSAT
150	10,636	10,723	10,516	10,587	11,325
200	10,528	10,449	10,552	10,359	11,120
250	10,325	10,139	10,298	10,320	11,034
300	11,070	11,186	11,147	11,150	11,595

Table 5: Analysis on transmission delay under Scenario 1.

Count of nodes	SA-DHO (Sumesha)	MIFA (Sumeshb)	SLO	CSA	CSUSAT
150	8.3289	8.6749	8.3199	8.3401	8.342
200	8.2642	8.5696	8.349	8.3791	8.3912
250	7.6938	8.0778	7.858	7.5866	7.7982
300	8.0147	8.1359	8.0234	7.9391	7.9191

Table 6: Analysis on transmission delay under Scenario 1.

Count of nodes	SA-DHO (Sumesha)	MIFA (Sumeshb)	SLO	CSA	CSUSAT
150	7.9168	8.4143	7.8518	7.8696	7.9667
200	7.8527	8.3147	7.9035	7.742	7.8409
250	7.8026	8.3339	7.7642	7.7785	7.6708
300	8.2466	8.6141	8.2789	8.2718	8.3082

Scenario 2, the proposed work is 20, 19, 17.5, 16.75% superior to existing models like SA-DHO (Sumesha), MIFA (Rehan et al. 2020), SLnO and CSA, respectively. From the analysis, it is clear that the proposed method is more energy-efficient and has a higher network lifetime.

Author contributions: All the authors have accepted responsibility for the entire content of this submitted manuscript and approved submission.
Research funding: None declared.
Conflict of interest statement: The authors declare no conflicts of interest regarding this article.

References

AlBalushi, F. M. 2019. "Chaotic Based Hybrid Artificial Sheep Algorithm – Particle Swarm Optimization for Energy and Secure Aware in WSN." *Journal of Networking and Communication Systems* 2 (2): 37–48.

Al-Zahrani, F. A. 2020. "On Modeling Optimizations and Enhancing Routing Protocols for Wireless Multihop Networks." *IEEE Access* 8: 68953–73.

Amit, K., and P. Pandey. 2019. "Energy-Aware Cluster Head Selection in WSN Using HPSOCS Algorithm." *Journal of Networking and Communication Systems* 2 (1): 24–33.

Aseri, T. C. 2013. "Performance Analysis of Cluster Based Routing Protocols in Heterogeneous Wireless Sensor Network." *International Journal of Computer Applications* 83 (16): 18–20.

Augustine, S., and J. P. Ananth. 2020. "Taylor Kernel Fuzzy C-Means Clustering Algorithm for Trust and Energy-Aware Cluster Head Selection in Wireless Sensor Networks." *Wireless Networks* 26: 5113–32.

Bhardwaj, R., and D. Kumar. 2019. "MOFPL: Multi-Objective Fractional Particle Lion Algorithm for the Energy Aware Routing in the WSN." *Pervasive and Mobile Computing* 58: 101029.

Bhardwaj, R., and D. Kumar. 2019. "Hybrid GSDE: Hybrid Grasshopper Self Adaptive Differential Evolution Algorithm for Energy-Aware Routing in WSN." *Journal of Networking and Communication Systems* 2 (4): 1–11.

Chang, C., and C. Tsai. 2019. "A Large-Scale Optical Fiber Sensor Network with Reconfigurable Routing Path Functionality." *IEEE Photonics Journal* 11 (3): 1–11.

Chithaluru, P., R. Tiwari, and K. Kumar. 2019. "AREOR–Adaptive Ranking Based Energy Efficient Opportunistic Routing Scheme in Wireless Sensor Network." *Computer Networks* 162: 106863.

Daneshvar, S. M. M. H., P. Alikhah Ahari Mohajer, and S. M. Mazinani. 2019. "Energy-Efficient Routing in WSN: A Centralized Cluster-Based Approach via Grey Wolf Optimizer." *IEEE Access* 7: 170019–31.

Darabkh, K. A., M. Z. El-Yabroudi, and A. H. El-Mousa. 2019. "BPA-CRP: A Balanced Power-Aware Clustering and Routing Protocol for Wireless Sensor Networks." *Ad Hoc Networks* 82: 155–71.

Darabkh, K. A., N. J. Al-Maaitah, I. F. Jafar, and A.' F. Khalifeh. 2018. "EA-CRP: A Novel Energy-Aware Clustering and Routing Protocol in Wireless Sensor Networks." *Computers & Electrical Engineering* 72: 702–18.

Darvishi, M., Y. Audet, Y. Blaquière, C. Thibeault, and S. Pichette. 2019. "On the Susceptibility of SRAM-Based FPGA Routing Network to Delay Changes Induced by Ionizing Radiation." *IEEE Transactions on Nuclear Science* 66 (3): 643–54.

Dattatraya, K. N., and K. Raghava Rao. 2020. "Hybrid FruitFly Optimization Algorithm and Wavelet Neural Network for Energy Efficiency in WSN." *Journal of Networking and Communication Systems* 3 (1): 41–9.

Fanian, F., and M. K. Rafsanjani. 2019. "Cluster-Based Routing Protocols in Wireless Sensor Networks: A Survey Based on Methodology." *Journal of Network and Computer Applications* 142: 111–42.

Fersi, G., W. Louati, and M. Ben Jemaa. 2016. "CLEVER: Cluster-Based Energy-Aware Virtual Ring Routing in Randomly Deployed Wireless Sensor Networks." *Peer-to-Peer Networking and Applications* 9: 640–55.

He, A., J. Long, and J. Zhang. 2019. "An Energy-Efficient Multi-Ring-Based Routing Scheme for WSNs." *IEEE Access* 7: 181257–72.

Huang, J., D. Ruan, and W. Meng. 2018. "An Annulus Sector Grid Aided Energy-Efficient Multi-Hop Routing Protocol for Wireless Sensor Networks." *Computer Networks* 147: 38–48.

Iztok, F., I. Fister Jr, X.-S. Yang, and B. Janez. 2013. "A Comprehensive Review of Firefly Algorithms." *Swarm and Evolutionary Computation* 13: 34–46.

Jacob, J., and P. Rodrigues. 2019. "Multi-Objective HSDE Algorithm for Energy-Aware Cluster Head Selection in WSN." *Journal of Networking and Communication Systems* 2 (3): 20–9.

Marsaline Beno, M., I. R. Valarmathi, S. M. Swamy, and B. R. Rajakumar. 2014. "Threshold Prediction for Segmenting Tumour from Brain MRI Scans." *International Journal of Imaging Systems and Technology* 24 (2): 129–37.

Mirjalili, S. 2015. "Moth-Flame Optimization Algorithm: A Novel Nature-Inspired Heuristic Paradigm." *Knowledge-Based Systems* 89: 228–49.

Movva, P., and P. T. Rao. 2019. "Novel Two-Fold Data Aggregation and MAC Scheduling to Support Energy Efficient Routing in Wireless Sensor Network." *IEEE Access* 7: 1260–74.

Mythili, V., A. Suresh, M. M. Devasagayam, and R. Dhanasekaran. 2019. "SEAT-DSR: Spatial and Energy Aware Trusted Dynamic Distance Source Routing Algorithm for Secure Data

Communications in Wireless Sensor Networks." *Cognitive Systems Research* 58: 143–55.

Pandiyaraju, V., R. Logambigai, S. Ganapathy, and A. Kannan. 2020. "An Energy Efficient Routing Algorithm for WSNs Using Intelligent Fuzzy Rules in Precision Agriculture." *Wireless Personal Communications* 112: 1–17.

Paul, B. 2020. "A Novel Energy-Efficient Routing Scheme for LoRa Networks." *IEEE Sensors Journal* 20 (15): 8858–66.

Pradeesha, P., G. Ravi, and P. Priya. 2019. "Ring Routing Clustering Based Energy Efficient Protocol for Wireless Sensor Networks." In *2019 5th International Conference on Advanced Computing & Communication Systems (ICACCS),* Coimbatore, India, 712–6. IEEE Conference: Coimbatore.

Rathod, S. 2020. "Hybrid Metaheuristic Algorithm for Cluster Head Selection in WSN." *Journal of Networking and Communication Systems* 3 (4): 101504.

Rehan, W., S. Fischer, M. Rehan, Y. Mawad, and S. Saleem. 2020. "QCM2R: A QoS-Aware Cross-Layered Multichannel Multisink Routing Protocol for Stream Based Wireless Sensor Networks." *Journal of Network and Computer Applications* 156: 102552.

Sarkar, A., and T. Senthil Murugan. 2019. "Adaptive Cuckoo Search and Squirrel Search Algorithm for Optimal Cluster Head Selection in WSN." *Journal of Networking and Communication Systems* 2 (3): 30–9.

Singh, D., and B. K. Pattanayak. 2017. "Performance Analysis of Shortest Time Regional Head Path Protocol (STRHP) in Wireless Sensor Networks." *Far East Journal of Electronics and Communication* 17 (6): 1515–40.

Sumesh. "Energy Efficient Secure-Trust Based Ring Cluster Routing in Wireless Sensor Network." (in communication).

Sumesh. "Energy Conserving Ring Cluster-Based Routing Protocol for Wireless Sensor Network: A Hybrid Based Model." (in communication).

Thangaramya, K., K. Kulothungan, R. Logambigai, M. Selvi, and A. Kannan. 2019. "Energy Aware Cluster and Neuro-Fuzzy Based Routing Algorithm for Wireless Sensor Networks in IoT." *Computer Networks* 151: 211–23.

Thirukrishna, J. T., S. Karthik, and V. P. Arunachalam. 2018. "Revamp Energy Efficiency in Homogeneous Wireless Sensor Networks Using Optimized Radio Energy Algorithm (OREA) and Power-Aware Distance Source Routing Protocol." *Future Generation Computer Systems* 81: 331–9.

Tunca, C., S. Isik, M. Yunus Donmez, and C. Ersoy. 2013. "Ring Routing: An Energy-Efficient Routing Protocol for Wireless Sensor Networks with a Mobile Sink." *IEEE Transactions on Mobile Computing* 14: 1947–60.

Vinitha, A., M. S. S. Rukmini, and Dhirajsunehra. 2019. "Secure and Energy Aware Multi-Hop Routing Protocol in WSN Using Taylor-based Hybrid Optimization Algorithm." *Journal of King Saud University – Computer and Information Sciences*, https://doi.org/10.1016/j.jksuci.2019.11.009 (in communication).

Vinusha, S., and J. S. Abinaya. 2018. "Performance Analysis of the Adaptive Cuckoo Search Rate Optimization Scheme for the Congestion Control in the WSN." *Journal of Networking and Communication Systems* 1 (1): 19–27.

Wang, J. 2020. "Hybrid Optimization Algorithm for Multihop Routing Protocol in WSN." *Journal of Networking and Communication Systems* 3 (3), https://doi.org/10.46253/jnacs.v3i3.a5.

Wu, H., F. Zhou, Z. Zhu, and Y. Chen. 2019. "Analysis Framework of RSA Algorithms in Elastic Optical Rings." *Journal of Lightwave Technology* 37 (4): 1113–22.

Yarinezhad, R., and S. N. Hashemi. 2019. "A Routing Algorithm for Wireless Sensor Networks Based on Clustering and an Fpt-Approximation Algorithm." *Journal of Systems and Software* 155: 145–61.

Yuan, Y., W. Liu, T. Wang, Q. Deng, A. Liu, and H. Song. 2019. "Compressive Sensing-Based Clustering Joint Annular Routing Data Gathering Scheme for Wireless Sensor Networks." *IEEE Access* 7: 114639–58.

Zhang, W., L. Li, G. Han, and L. Zhang. 2017. "E2HRC: An Energy-Efficient Heterogeneous Ring Clustering Routing Protocol for Wireless Sensor Networks." *IEEE Access* 5: 1702–13.

Zhang, W., X. Wei, G. Han, and X. Tan. 2018. "An Energy-Efficient Ring Cross-Layer Optimization Algorithm for Wireless Sensor Networks." *IEEE Access* 6: 16588–98.

Zhu, D., H. Zhu, X. Liu, H. Li, F. Wang, H. Li, and D. Feng. 2020. "CREDO: Efficient and Privacy-Preserving Multi-Level Medical Pre-Diagnosis Based on ML-kNN." *Information Sciences* 514: 244–62.